Supplementary Information (SI) for Nanoscale Horizons.
This journal is © The Royal Society of Chemistry 2025

Supporting Information

Transferrin-Targeted Nanoplatform for MRI-Guided Visualization and Potent Suppression of Tumors and Pulmonary Metastatic Lesion

Liya Tian[a†], Pengju Ma[b†], Wenxiu Zhuang[b], Yinlong Xu[c], Lihua Pang[b], Kai Guo[a], Ren Ke[a], Xueli Xu[b], Xiao Sun*[a], Shunzhen Zheng*[c]

[a]Medical Science and Technology Innovation Center, Shandong Cancer Hospital and Institute, Shandong First Medical University & Shandong Academy of Medical Sciences, Jinan 250000, China
[b]School of Science, Shandong Jianzhu University, Jinan, 250101, China
[c]Department of Hepatobiliary Surgery, Shandong Provincial Hospital Affiliated to Shandong First Medical University, Jinan 250021, China

E-mail addresses: sunxiao@sdfmu.edu.cn (X. Sun), zsz5512920@hotmail.com (S. Zheng)

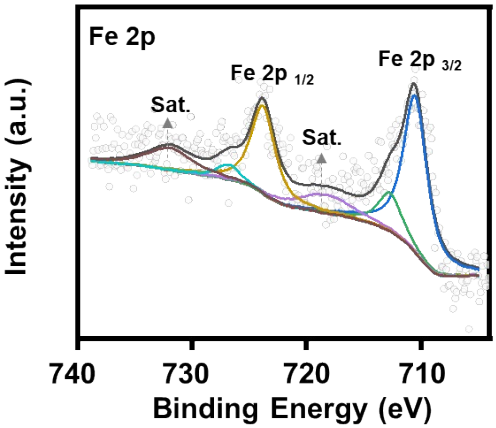

Figure S1. XPS spectra of the Fe 2p regions.

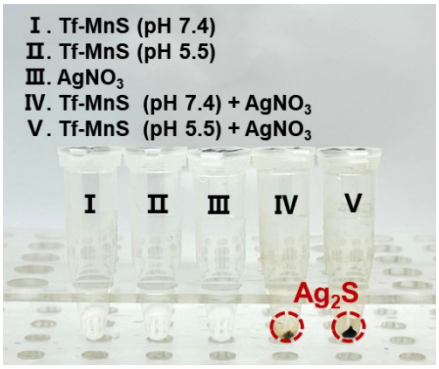

Figure S2. Images of detecting H_2S generated by Tf-MnS at different pH values using silvernitrate ($AgNO_3+H_2S \rightarrow Ag_2S$).

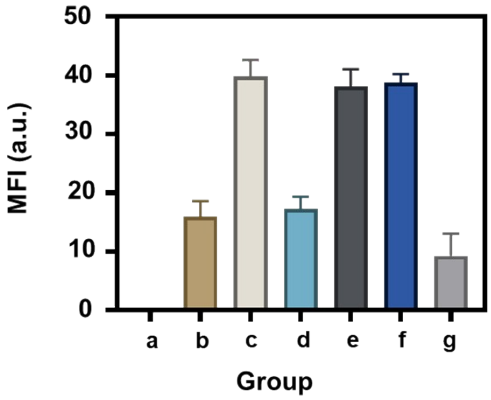

Figure S3. The corresponding statistical data of cellular uptake. (a.Tf-MnS 0 μg/mL, b. Tf + Tf-MnS 40 μg/mL, c. Tf-MnS 40 μg/mL, d. M-β-CD + Tf-MnS 40 μg/mL, e. CPZ + Tf-MnS 40 μg/mL, f. AMR + Tf-MnS 40 μg/mL, g. 4℃ + Tf-MnS)

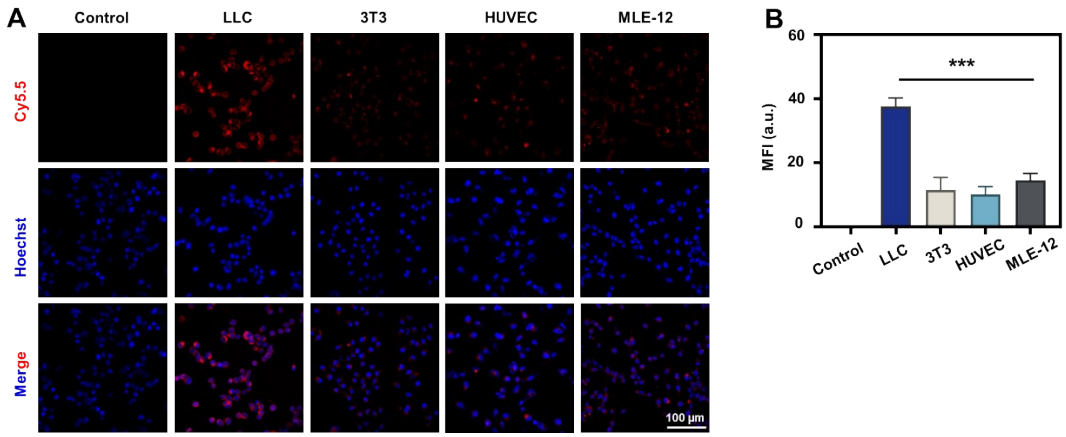

Figure S4. (A) CLSM observation of cellular uptake of Tf-MnS in different cell types and (B) corresponding statistical data (n=3, ***p < 0.001).

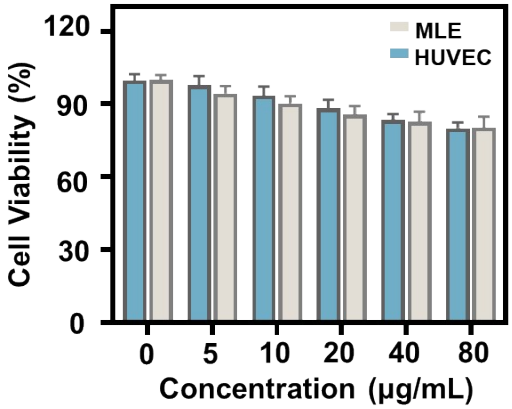

Figure S5. Cell viability of MLE cells and HUVEC treated by Tf-MnS.

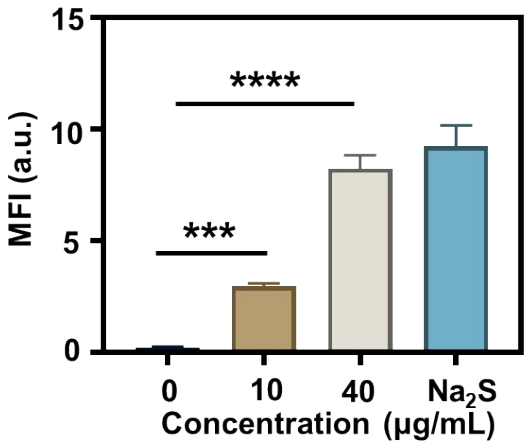

Figure S6. Quantification of mean fluorescence intensity (MFI) for H_2S production.

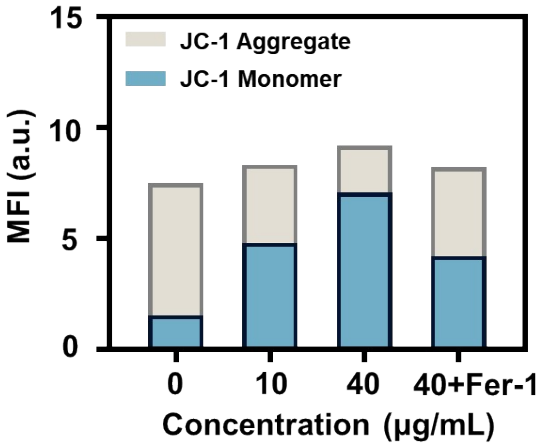

Figure S7. Quantification of MFI for JC-1.

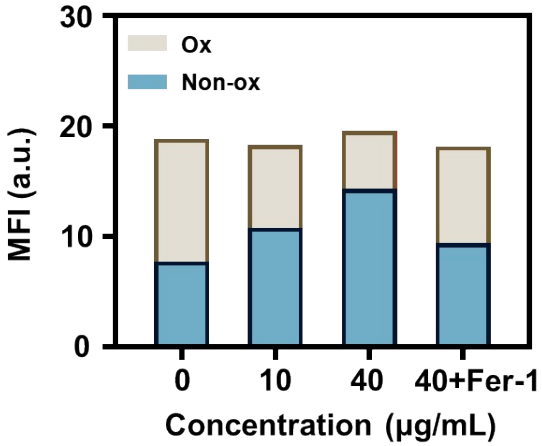

Figure S8. Quantification of MFI for C11- BODIPY.

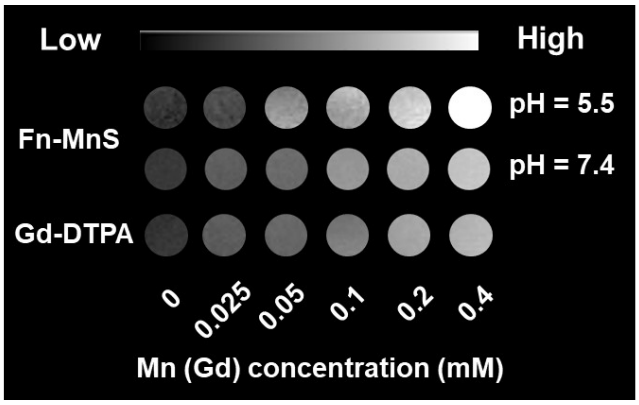

Figure S9. T_1-weighted MR images of agarose gels containing Tf-MnS and Gd-DTPA.

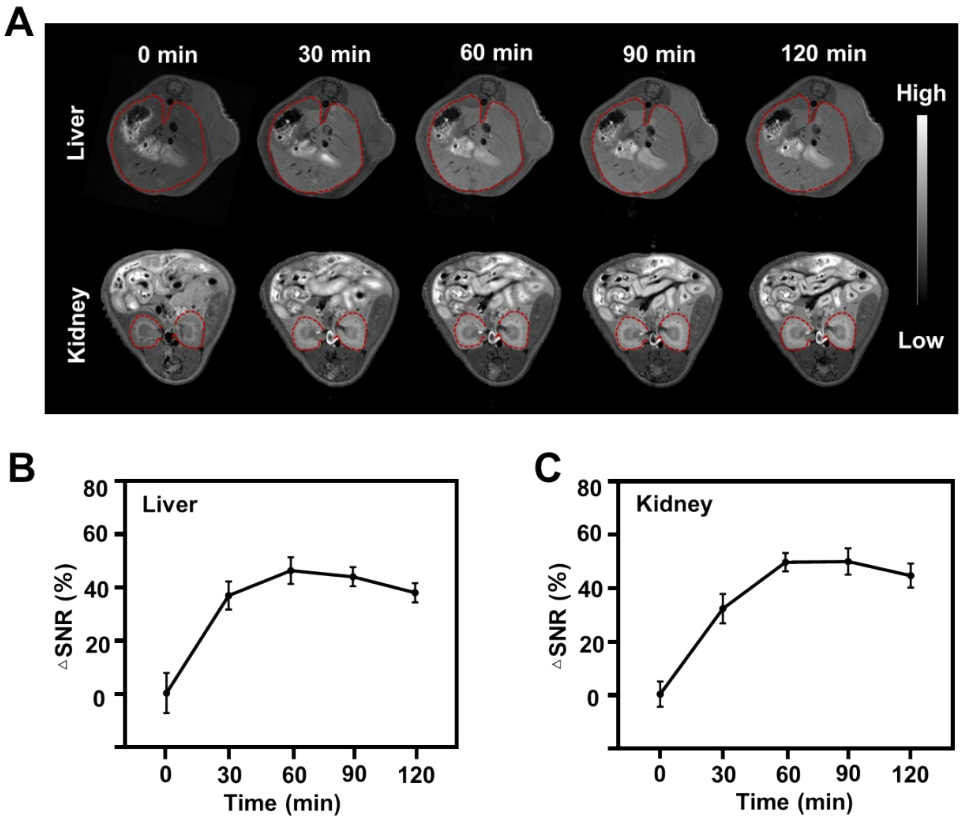

Figure S10. (A) MR images after intravenous injection of Tf-MnS, and the dashed red circles indicated liver and kidney. (B) and (C) Comparative analysis of the change in ΔSNR of liver and kidney.

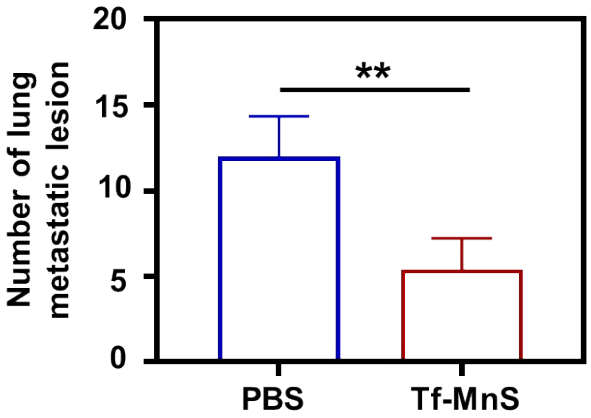

Figure S11. The number of visible lung metastatic lesion in each group (n=5, **p < 0.01).

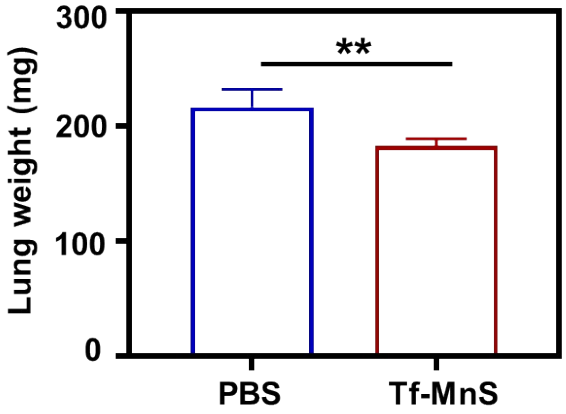

Figure S12. Lung weight of excised lungs in each group (n=5, **p < 0.01).

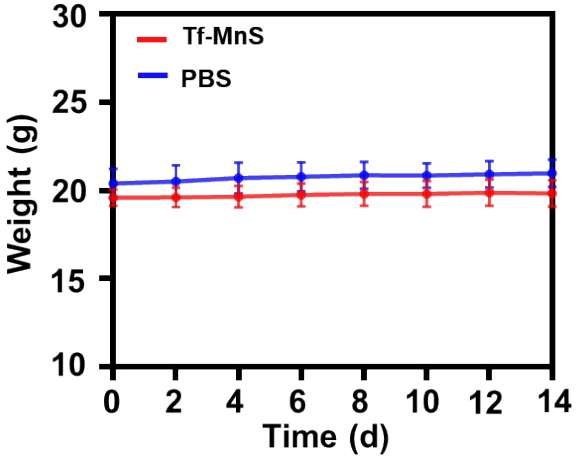

Figure S13. Body weight changes in tumor-bearing mice subjected to various treatments were recorded bi-daily.

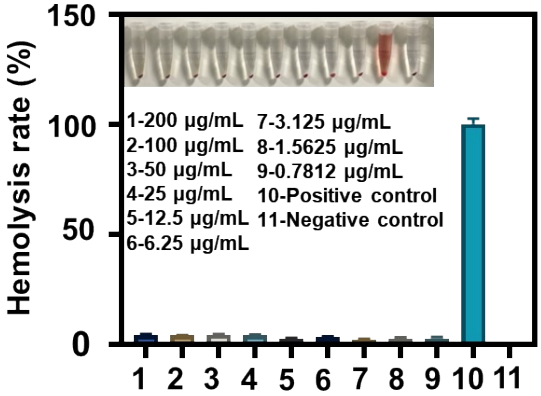

Figure S14. Hemolysis assay with different concentration of Tf-MnS.